Acta Crystallographica Section A
Foundations of Crystallography
ISSN 0108-7673

Received 25 July 2001
Accepted 17 September 2001

Lattice-parameter determination from the interaction of short femtosecond laser pulses with crystalline solids

R. Ondarza-Rovira

Instituto Nacional de Investigaciones Nucleares, Departamento de Física, AP 18-1027, México 11801, DF, Mexico. Correspondence e-mail: ondarza@nuclear.inin.mx

A novel method for determining the lattice parameter in a crystalline solid from the harmonic emission spectra reflected in laser–solid layers interactions is proposed. Radiated emission at high-order harmonic numbers is observed from thin crystalline layers illuminated by short femtosecond elliptically polarized laser light. The radiation mechanism presented here accounts for optical emission effects when free electrons in the material, ionized by the action of an applied external radiation field, are driven to large oscillation amplitudes and harmonics are generated by the electronic response to the periodic lattice potential. Perturbations in the electron motion inside the material due to the ion cores give rise to harmonic emission. In this work, the condition for radiation – the resonance condition – is found analytically through an exact expression for the electron displacement. The analytic prediction is supported by results obtained by solving numerically the electromagnetic force equations for electrons moving in the lattice potential.

1. Introduction

Crystalline structure has been one of the main subjects studied in most of the usual applications of metals and ceramics (Ziman, 1972) and even in newly developed nanostructured arrays (Gutiérrez-Wing *et al.*, 2000; Wang, 1998; Wales, 1996). In all these cases, the study of the cell parameters has become of major importance for the determination of properties from the atomic ordering to macroscopic scales, as found in optical emission and conductivity, among many others (Bragg, 1947). Electron and neutron diffraction and X-ray techniques have been widely used in materials science to determine the physical properties and the structure of lattice arrays (Booker, 1969; Williams & Carter, 1996; Bacon, 1975; Giacovazzo *et al.*, 1995). In this work, we propose a laser application as a novel and alternative method for determining the lattice parameter in a crystalline solid.

As will be discussed later, the emission from crystals studied here is a surface effect, with the implication that the different detection methods present distinct conditions for their application. In the first place, even though neutron diffraction can provide high accuracy, neutron fluxes and crystals with dimensions of several millimetres in thickness are required for measuring appreciable scattered intensities, with disadvantages in the experimental costs. For electron diffraction, the resolution that can be achieved is equivalent, for instance, to 2 Å at an acceleration potential of 100 kV and is convenient for studying processes in the crystal surfaces such as electronic and ionic emission, catalysis, nucleation of phases and oxidation for low energies, and order–disorder phenomena, grain boundaries and structure of crystals for high-energy diffraction. Electron diffraction is particularly favourable for studying point defects in crystals. Lastly, X-ray diffraction can be used to study specimens which are of the order of millimetres in thickness, taking minutes or hours to record data unless a synchrotron or a sensitive detector is used for quantifying the number of photons. With this technique, high values of $\sin\theta/\lambda_L$, where λ_L is the laser wavelength, can draw fine details of crystalline structures of sizes $\sim$0.5 Å.

On the other hand, the method proposed in this work would have the drawback that when using an ultrashort laser pulse the incident radiation would not be really monochromatic and spectral broadening would have to be taken into consideration. However, for 9.5 µm femtosecond mid-infrared pulse production ($\sim$100 fs), it has been shown in the experiment that the power spectra is broadened with a width of $\Delta\lambda_L \simeq 1$ µm (FWHM) (Rolland & Corkum, 1986). From those results, we estimated numerically the location of the strong emission peaks in the spectra (a distinctive feature, as we will see later) for deviations of $\pm$0.5 µm for a CO_2 laser wavelength and found that the lattice parameter could be measured with an error below 10% of the real value for both linear and circular polarizations. The emission effect, if detected in-laboratory, would represent a direct method for determining the lattice parameter at a low cost and with an acceptable approximation.

Recent work on emission phenomena from the irradiation of thin solid layers by short-pulse lasers has revealed that high-order harmonic emission can be generated (Hüller & Meyer-

ter-Vehn, 1993; Ondarza, 1998). The model, proposed from results reported by Hüller & Meyer-ter-Vehn (1993) and extended by Ondarza (1998), describes the emission mechanism in terms of the motion of ionized electrons – driven by the applied external radiation field – in the crystalline layer and perturbed by the action of the ion lattice potential. Harmonic emission arises from perturbation effects produced on the electron dynamics. It was shown that the radiated emission spectra are distinguished by characteristic and prominent harmonic lines. In particular, for linearly polarized laser light incident on a periodic ion array, the emission was found to be characterized by a spectral region that forms a plateau over the lower harmonic numbers with a sudden cutoff for the highest orders. It was found that the maximum harmonic number emitted depends mainly on the strength and the wavelength of the driver and on the lattice spacing. In this work we obtain in analytical form the condition for radiation – the resonance condition – derived on the basis of conservation laws for the momentum and the energy when an elliptically polarized laser pulse is incident on a crystalline layer.

Harmonic generation from solids illuminated by laser light can be produced from a number of distinct physical processes. We briefly review some relevant results, remarking that the input energies and shortness of the pulse used in those reports are not applicable in our model.

Strong emission from solid targets irradiated by nanosecond CO_2 lasers with intensities $>5 \times 10^{14}$ W cm^{-2} was first observed by Carman, Forslund & Kindel (1981) and Carman, Rhodes & Benjamin (1981), who detected up to 46 harmonics. Other experiments have confirmed harmonic generation from solid targets with laser pulses of duration from hundreds of femtoseconds up to a few picoseconds (Linde *et al.*, 1995; Kohlweyer *et al.*, 1995; Norreys *et al.*, 1996). The first of these reported emission up to the seventh harmonic from 150 fs, 0.794 μm laser pulses at intensities of 10^{19} W cm^{-2}, while the second detected up to 15 harmonics for 0.8 μm, 130 fs lasers at 10^{17} W cm^{-2}. The work by Norreys *et al.* (1996) found harmonic emission up to the 75th order from 1.053 μm pulses of 2.5 ps at 10^{19} W cm^{-2}.

The radiation phenomena studied in this work present features in common with emission effects generated when charged particles traverse an inhomogeneous medium. In particular, the emission mechanism considered here resembles the Smith–Purcell (SP) effect (Smith & Purcell, 1953; Moran, 1992; Doucas *et al.*, 1992; Hüller & Meyer-ter-Vehn, 1993), an effect independently found by Salisbury (1953), in which radiated light arises when highly energetic electrons, with energies above 50 keV, pass over a periodical array of grooves in the surface of a metallic grating. Coherent band radiation is emitted in the SP effect in the radio to ultraviolet range with frequencies $\omega = \mathbf{k}_g \cdot \mathbf{v}\,(1 - \beta\cos\theta)^{-1}$, where $\mathbf{k}_g$ is the grating periodicity, $\mathbf{v}$ stands for the beam electron velocity, $\beta = v/c$, and θ is the angle between the beam direction and the source–observer axis.

In §2, we briefly account for considerations and aspects of the interaction of laser pulses with a lattice array. §3 solves numerically the electron dynamics and presents the emission spectra for different laser intensities. In §4, the analytical solution for the motion of electrons driven by an electromagnetic elliptically polarized laser field is obtained. The condition of resonance is also obtained from the equations for the electron displacement. Finally, §5 draws conclusions from the work performed.

2. Interaction of a laser pulse with a periodic lattice

This section accounts for some aspects of the interaction physics of ionized electrons driven by laser light in a crystalline array. The transverse quiver momentum of an electron embedded in a light field is given by $\mathbf{p} = m_0 c\mathbf{a}_0$, where $\mathbf{a}_0 = e\mathbf{A}_0/m_0c^2$ is the normalized vector potential and e, c, m_0 and $\mathbf{A}_0$ stand for the electron charge, the speed of light in vacuum, the electron rest mass and the vector potential, respectively. For incident light of wavelength λ_L (in micrometres) and intensity I_{18} (in units of 10^{18} W cm^{-2}), the magnitude of the normalized vector potential can be denoted as $a_0 \simeq 0.8544\,(I_{18})^{1/2}\,\lambda_L$. At high intensities, the crystalline structure can be distorted by the action of the driver producing alterations in the periodicity of the electron motion. Nevertheless, the lattice structure can preserve its initial configuration when ultrashort and low-intense laser pulses are applied. It has been shown from a number of experimental works that ultrashort femtosecond laser pulses of intensities lower than 10^{11} W cm^{-2} can be applied without impinging important damage on a crystalline structure (Silvestrelli *et al.*, 1996; Sokolowski-Tinten *et al.*, 1998). Laser-induced disorders of material surfaces for laser pulses of several hundreds of femtoseconds duration at peak intensities of tenths of J cm^{-2} have been observed (Tom *et al.*, 1988; Saeta *et al.*, 1991) where a loss of cubic order was found 150 fs after the pulse.

Alternatively, lattice dynamics can be studied by ultrafast optical spectroscopic techniques. For instance, chemical bonds in crystal lattices have been observed to rearrange on time scales of femtoseconds to picoseconds. With the use of time-resolved generation of ultrashort X-ray pulses, it has been possible to observe fundamental processes such as electronic changes and coherent acoustic phonon propagation through optical excitation of the crystal surface (Rose-Petruck *et al.*, 1999). Direct observation of optically induced phase transitions in crystals (InSb) has been reported from 150 fs, 0.8 μm laser pulses above critical fluences of 13 mJ cm^{-2} (Lindenberg *et al.*, 2000), and interpreted as lattice atomic motion driven from equilibrium to disordered states.

Ultrashort laser pulses can be used to excite the electronic states of a solid before tangible energy is deposited to the lattice vibrational states. Second-harmonic generation (SH) experiments (Shank *et al.*, 1983) on laser irradiation on crystals have confirmed that emission from the surface layer dominates that from the bulk, allowing SH to be successfully used to study molecular adsorption and orientation on surfaces (Tom *et al.*, 1984). The proposed method for determining the lattice structure from solids is basically a surface effect where the shortness of the pulse enables interaction

with the surface without producing distortions in the crystalline array.

The mechanism of radiation discussed here might be expected to be screened by other effects concerning multiphoton processes and atomic emission from recombination and line transitions. Nevertheless, those effects can be discerned since they take place on longer time scales, as compared with the emission that would be generated from electrons perturbed by the lattice potential.

Taking the above into consideration, in our simulations of laser–target interactions we have used CO_2 laser light (λ_L = 10.6 μm) with a pulse duration of only a few femtoseconds, allowing quiver excursions $\delta = (\lambda_L/2\pi)a_0$ greater than the lattice spacing l_c. For instance, for $I_L = 5 \times 10^{10}$ W cm^{-2} ($a_0 \simeq 2.025 \times 10^{-3}$), the lattice electrons execute oscillation amplitudes of $\delta/l_c \simeq 9$.

Laser technology capable of delivering CO_2 light pulses of only 2 ps duration was first developed from optical semiconductor switching (Corkum, 1983, 1985) where compression was performed by a technique consisting of plasma chirping and anomalous dispersion. Many potential applications, including multiphoton chemistry and plasma physics, provided interest for pursuing the construction of such devices.

Subsequent developments allowed infrared pulses of duration 130 fs based on such techniques to be achieved inlaboratory (Rolland & Corkum, 1986). Such pulses contained only about four optical cycles. An important aspect associated with ultrashort pulses is that the broadening of the spectrum of the driver covers a wide range of wavelengths. From the analyses of the power spectra, the radiation at the incident CO_2 wavelength dominates, with weak emission at the blue and red wings. Minor modifications in the experimental set-up could produce developments in the amplification of ultrashort pulses of duration equal to (or even smaller than) the visible light (35 fs) used to produce the pulse (Knox, 1988). Taking this into account, the prospect of achieving shorter pulses of one optical cycle is feasible. Optical semiconductor switching for wavelengths longer than 30 μm could still be implemented for many laboratory applications. For our model, such lasers could be employed in even lower energy ranges, from 5×10^7 to 10^8 W cm^{-2}.

We represent the lattice potential by assuming a periodic function of the coordinates. In this work, we consider a two-dimensional lattice potential in the form

$$\varphi(\mathbf{r}) = \varphi_c \sinh[A \sin(\mathbf{k}_c \cdot \mathbf{r})], \qquad (1)$$

where $k_c = 2\pi/l_c$ is the lattice wavelength, and the strength of the amplitude φ_c is of the order of 1 V for typical metals (Pettifor, 1983). The factor A in the expression above has been incorporated into the model with the aim of including variations in the lattice potential. Such variations can be produced in cases where impurities or interstitial sites occur in the crystal. In this work, we take the value $A = 1$ to represent the lattice force as the conventional sinusoidal function and leave those cases in which A takes other values for a future publication. For the case of linear polarization, the electrons quiver in the direction of oscillation of the laser electric field reducing the mode to one dimension. For circularly polarized laser fields, the electrons describe periodic oscillations in the plane perpendicular to the direction of propagation of the pulse. For this polarization, the resonance condition (as we will see in the following section) will be mainly given in terms of the electron displacements in that plane and the small drifts along the Poynting vector will have a negligible contribution for determining the lattice parameter. Fig. 1 shows the lattice potential for a two-dimensional ion array.

3. Harmonic emission spectra from crystalline targets

The radiation emission spectra reflected from the target were obtained by studying the dynamics of the electrons. A single-particle force equation was solved numerically for an elliptically polarized laser field incident on the target,

$$\frac{\mathrm{d}\mathbf{p}}{\mathrm{d}t} = -e\mathbf{E} - (e/c)\,\mathbf{v} \times \mathbf{B} + e\nabla\varphi,$$

where φ is the lattice potential given by (1), e is the charge of the electron and c is the velocity of light in vacuum, $\mathbf{p} = m_0\mathbf{v}\gamma$ is the electron momentum with $\gamma = (1 - v^2/c^2)^{-1/2}$. $\mathbf{E}$ and $\mathbf{B}$ are the electric and magnetic fields, respectively. For a monochromatic plane wave of arbitrary polarization propagating along the x direction, the vector potential can be written as

$$\mathbf{A}(\mathbf{r}, t) = a(\eta)\mathbf{A}(\eta),$$

where $a(\eta)$ is a shape factor and

$$\mathbf{A}(\eta) = \left[0, (1 - \delta^2)^{1/2} \sin\eta, \delta\cos\eta\right].$$

The Lorentz invariant phase is denoted by $\eta = w_L(t - x/c)$. The parameter δ takes the values $\delta = 0, \pm 1$ for linear polarization and $\delta = \pm 1/2^{1/2}$ for circular polarization. Pulse shape effects will be studied in a future publication. In this paper, we consider, simplistically, ultrashort finite laser pulses interacting with thin solid targets.

We have considered a number of laser–target interactions with lattice period $l_c = 4$ Å and different laser intensities.

The power radiated by single electrons per unit solid angle in a direction $\mathbf{\Omega}$ is given by (Jackson, 1962)

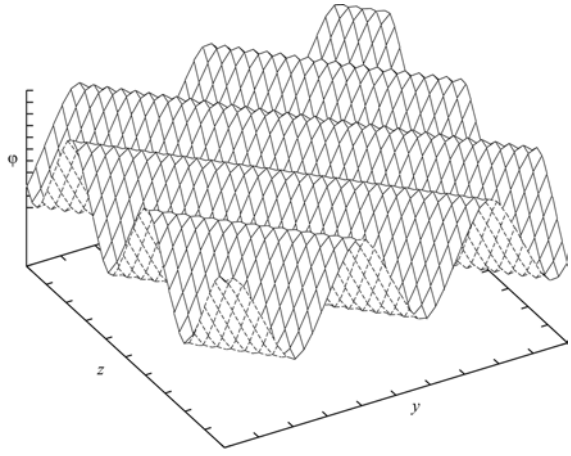

Figure 1
Lattice force as represented by equation (1).

$$\frac{\mathrm{d}P(t)}{\mathrm{d}\Omega} = (c/4\pi)\left|R\,\mathbf{E}_{\mathrm{rad}}(t,\Omega)\right|^2,$$

where

$$\mathbf{E}_{\mathrm{rad}}(t,\Omega) = -(e/c^2)\;\boldsymbol{\Omega}\times[\boldsymbol{\Omega}\times\ddot{\mathbf{r}}\,(t')]/R,$$

where $R = |\mathbf{R}_{\mathrm{obs}} - \mathbf{r}|$ and $t' = t - \boldsymbol{\Omega}\cdot(\mathbf{R}_{\mathrm{obs}} - \mathbf{r})/c$ is the retarded time.

For a linearly polarized laser pulse, Fig. 2 shows the radiation spectrum for a laser light of λ_L = 10.6 µm and I_L = 5×10^9 W cm^{-2}. This figure shows that the spectrum is characterized by a well defined plateau with a cutoff around m = 16. Here, m denotes the harmonics $\omega_m = m\omega_L$. The emitted power is normalized by a factor $f_n = 4.7\times10^{-14}$, and where the fundamental is not shown for convenience in the power scale.

For a solid layer illuminated by a circularly polarized laser pulse, Figs. 3 and 4 show the emission for a laser pulse of intensity $I_L = 5\times10^9$ and $I_L = 5\times10^{10}$ W cm^{-2}, respectively. In both cases we observe that the emission presents an additional peak in the region of low harmonic orders with a plateau between the two maxima emitted. In Fig. 3, two peaks are strongly emitted around m = 8 and m = 31 with f_n = 1.9×10^{-13}. For Fig. 4, the peaks are around m = 25 and m = 100 with $f_n = 2.9\times10^{-12}$.

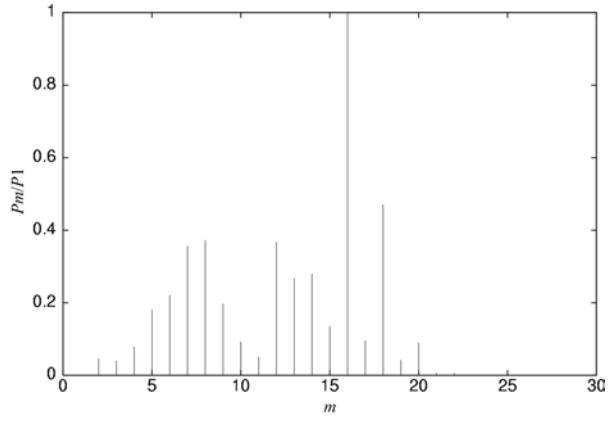

Figure 2
Radiation spectrum for linear polarization, $I_L = 5\times10^9$ W cm^{-2}, λ_L = 10.6 µm and l_c = 4 Å.

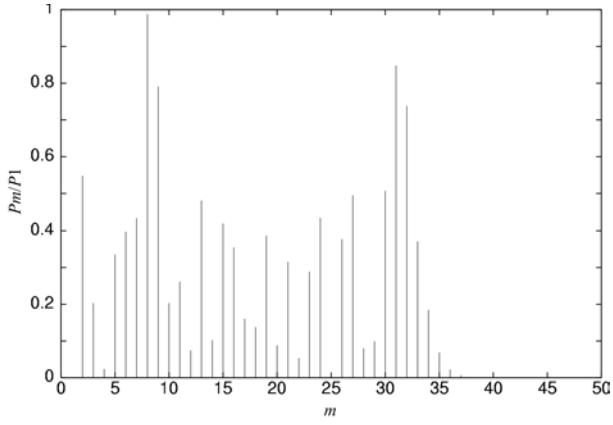

Figure 3
Radiation spectrum for circular polarization, $I_L = 5\times10^9$ W cm^{-2}, λ_L = 10.6 µm and l_c = 4 Å.

4. Resonance condition for radiation

With the aim of obtaining the resonance condition for radiation and, from that condition, the lattice parameter of a crystalline target, we solve analytically the motion of free charged particles driven by an external elliptically polarized laser field without the action of other external sources (Ondarza, 2001).

From the equation of motion we have

$$\begin{aligned}\frac{\mathrm{d}}{\mathrm{d}t}(\gamma v_y) &= -a_0 c(1-\delta^2)^{1/2}\dot{\eta}\cos\eta,\\ \frac{\mathrm{d}}{\mathrm{d}t}(\gamma v_z) &= a_0 c\delta\dot{\eta}\sin\eta,\end{aligned} \tag{2}$$

where $\dot{\eta} = \omega_L[1-(v_x/c)]$. On the other hand, we have that

$$\frac{\mathrm{d}}{\mathrm{d}t}(\gamma v_x) = \frac{\mathrm{d}}{\mathrm{d}t}(\gamma c) = a_0\omega\left[v_z\delta\sin\eta - v_y(1-\delta^2)^{1/2}\cos\eta\right],$$

from which we obtain

$$\gamma = [1-(\dot{x}/c)]^{-1} = (p_x + m_0 c)/m_0 c. \tag{3}$$

Using the equation for the energy, $E = m_0\gamma c^2 = p^2c^2 + m_0^2c^4$, the expression for γ and (2), we get

$$\begin{aligned}p_x &= (a_0^2 m_0 c/2)\left[(1-\delta^2)\sin^2\eta + \delta^2(1-\cos\eta)^2\right],\\ p_y &= -m_0 a_0 c(1-\delta^2)\sin\eta,\\ p_z &= m_0 a_0 c\delta(1-\cos\eta).\end{aligned}$$

Expressing the velocities in the form

$$v_i = \frac{\mathrm{d}i}{\mathrm{d}\eta}\dot{\eta},\quad i = x, y, z,$$

and upon integration we have

$$i = (1/m_0\omega)\int p_i\,\mathrm{d}\eta,\quad i = x, y, z.$$

After integration we obtain

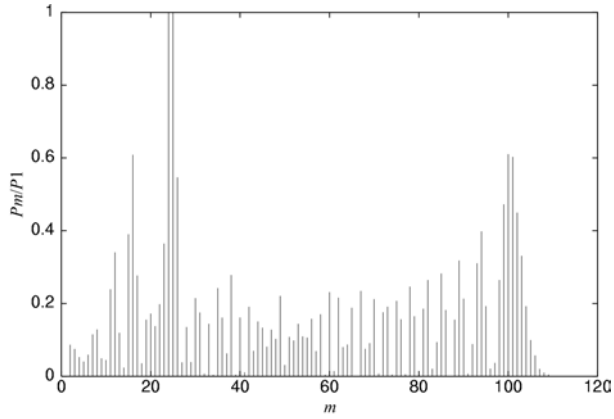

Figure 4
Radiation spectrum for circular polarization, $I_L = 5\times10^{10}$ W cm^{-2}, λ_L = 10.6 µm and l_c = 4 Å.

$$x = (a_0^2/2k)\left\{\tfrac{1}{2}(2\delta^2+1)\eta + [(\sin 2\eta)/4](2\delta^2-1) - 2\delta^2 \sin\eta\right\},$$
$$y = -(a_0/k)(1-\delta^2)^{1/2}(1-\cos\eta),$$
$$z = (a_0/k)\delta(\eta - \sin\eta),$$

which are the expressions for the coordinates in terms of the Lorentz invariant phase η.

For linear polarization ($\delta = 0$), we have

$$\begin{aligned} x &= (a_0^2/4k)[\eta - (\sin 2\eta)/2], \\ y &= -(a_0/k)(1-\cos\eta), \\ z &= 0. \end{aligned} \tag{4}$$

For circular polarization ($\delta = 2^{-1/2}$), the spatial coordinates are given by the set of equations

$$\begin{aligned} x &= (a_0^2/2k)(\eta - \sin\eta), \\ y &= -(a_0/2^{1/2}k)(1-\cos\eta), \\ z &= (a_0/2^{1/2}k)(\eta - \sin\eta). \end{aligned} \tag{5}$$

The radiation spectrum produced when a charged particle moves in the vicinity of a periodic structure can be explained from conservation laws. Radiation arises only if resonance conditions are fulfilled. To explain this statement, let us assume that the medium changes its properties periodically along a certain direction. If we consider a particle travelling through a medium with velocity v and emitting quanta of energy $\hbar\omega$ and momentum $\hbar\omega/c$, the conservation laws for the longitudinal momentum and the energy can be written in general form as

$$(\mathbf{v}\cdot\delta\mathbf{p})/v - (\hbar\omega/c)\cos\theta' = 2\pi n/l,$$
$$\delta E - \hbar\omega = 0,$$

where θ' is the angle between the direction of an emitted quantum and the velocity $\mathbf{v}$. The changes in energy and momentum of the particle are denoted by δE and $\delta\mathbf{p}$, respectively, n is an arbitrary integer and l is the periodicity of the medium. Since $\delta E = \mathbf{v}\cdot\delta\mathbf{p}$ for small changes of the energy of the particle, the condition for radiation from the conservation laws reads

$$\omega_{\rm eff}/v \equiv (\omega/v)[1 - (v/c)\cos\theta'] = 2\pi n/l.$$

Thus, the location of the cutoff can then be derived from the resonance condition $n_{\max}\omega_L \simeq k_c v_{\rm osc}$, or $n_{\max} \simeq k_c\delta_{\rm osc}$, where $\delta_{\rm osc}$ is the electron displacement. In a similar way, we can locate the cutoff in the emission spectra from the amplitudes of the electron excursions for all three spatial directions. The cutoff, which corresponds to a maximum displacement in a given direction, is expressed as

$$n_{\max,i} = 2\pi\delta_i/l_c, \quad i = x, y, z,$$

where l_c is the lattice spacing and δ_i is the amplitude of the electron excursion for a particular coordinate. From the linear parts of (4) and (5), the amplitude of the excursions can be obtained by taking $\eta = \pi/2$, which corresponds to the value of the phase η for maximum amplitude in the electron quiver motion in the y direction.

For linear polarization, the electron displacements are given by

$$\begin{aligned} \delta_x &= \lambda_L a_0^2/8, \\ \delta_y &= \lambda_L a_0/2\pi, \\ \delta_z &= 0. \end{aligned} \tag{6}$$

Since δ_x is an order of magnitude smaller in a_0 than the displacement in y, we have that $n_{\max} = (2\pi/l_c)\delta_y$, yielding

$$l_c = 2\pi\delta_y/n_{\max} = \lambda_L a_0/n_{\max}. \tag{7}$$

For the case of Fig. 2, $n_{\max} \simeq 60$, for which $l_c \simeq 3.70$ Å. This value is close to that used for the lattice parameter ($l_c = 4$ Å) in the simulations.

For a circularly polarized laser pulse we have that

$$\begin{aligned} \delta_x &= \lambda_L a_0^2/8, \\ \delta_y &= \lambda_L a_0/(2\times 2^{1/2}\pi), \\ \delta_z &= \lambda_L a_0/(4\times 2^{1/2}). \end{aligned}$$

From these quantities, it is possible to derive the location of the emission peaks in the radiation spectra since they correspond to the coupling effect between these different oscillations modes. Since δ_x is an order of magnitude smaller in a_0 than the displacement in the other two directions, we have that two main modes will contribute to the emission peaks, and will be given by

$$n_{\max_+} = (2\pi/l_c)(\delta_z + \delta_y),$$
$$n_{\max_-} = (2\pi/l_c)(\delta_z - \delta_y).$$

Substituting the values for δ_z and δ_y in the equation above, we have that

$$l_c = (\lambda_L/n_{\max_\pm})[a_0/(2\times 2^{1/2})](\pi \pm 2). \tag{8}$$

Thus, the lattice parameter can be calculated by taking any of the values of $n_{\max_\pm}$ in the emission spectrum. For instance, for $I_L = 5\times 10^9$ W cm^{-2} ($a_0 \simeq 6.4\times 10^{-4}$), $n_{\max_+} = 31$ and $n_{\max_-} = 8$, as obtained from the numerical computation of the dynamic equations and shown in Fig. 3. These values yield $l_c = 3.9$ and 3.6, respectively, for the lattice parameter. For an intensity of 5×10^{10} W cm^{-2} ($a_0 \simeq 2.025\times 10^{-3}$), $n_{\max_+} = 100$ and $n_{\max_-} = 25$, as shown in Fig. 4, giving $l_c = 3.9$ and 3.5, respectively. The small contribution effect to the coupling from δ_x would be given by $(\pi/4)(\lambda_L/l_c)a_0^2$, with negligible values 0.0085 and 0.079 for the intensities 5×10^9 and 5×10^{10} W cm^{-2}, respectively.

5. Conclusions

A novel method for determining the lattice parameter by means of the radiation emission reflected from crystalline layers illuminated by laser pulses has been presented. For linearly polarized laser light, the emission spectra were found to be characterized by high-order harmonic numbers with a plateau and a sudden cutoff. For elliptically polarized light incident on a periodic lattice array, the spectra contained two strong emission peaks. It was found from the analytical solu-

tions that coupling effects between the modes that correspond to the excursion amplitudes contribute to that sort of emission. The resonance condition for radiation was derived from the electron displacements in all three spatial coordinates. For a given polarization, it was found that the lattice parameter can be determined analytically from the maxima in the emission spectra, which was linearly dependent on both the wavelength and the amplitude of the laser pulse. The emission effect discussed in this work, if detected, might hold some potential as a diagnostic and could be used to determine the structure characteristics of irradiated targets.

The author acknowledges financial support from Consejo Nacional de Ciencia y Tecnología (CONACyT) under contract No. 33251-E.

References

Bacon, G. E. (1975). *Neutron Diffraction.* Oxford: Clarendon Press.

Booker, G. R. (1969). *Modern Diffraction and Imaging Techniques in Material Sciences.* Amsterdam: North Holland.

Bragg, W. L. (1947). *The Crystalline State.* London: G. Bell and Sons.

Carman, R. L., Forslund, D. W. & Kindel, J. M. (1981). *Phys. Rev. Lett.* **46**, 29–32.

Carman, R. L., Rhodes, C. K. & Benjamin, R. F. (1981). *Phys. Rev. A*, **24**, 2649–2663.

Corkum, P. B. (1983). *Opt. Lett.* **8**, 514–516.

Corkum, P. B. (1985). *IEEE J. Quantum Electron.* **21**, 216–232.

Doucas, G., Mulvey, J. H., Omori, M., Walsh, J. & Kimmitt, M. F. (1992). *Phys. Rev. Lett.* **69**, 1761–1764.

Giacovazzo, C., Monaco, H. L., Viterbo, D., Scordari, F., Gilli, G., Zanotti, G. & Catti, M. (1995). In *Fundamentals of Crystallography*, edited by C. Giacovazzo. Oxford University Press.

Gutiérrez-Wing, C., Santiago, P., Ascencio, J. A., Camacho, A. & José-Yacamán, M. (2000). *Appl. Phys.* A**71**, 237–243.

Hüller, S. & Meyer-ter-Vehn, J. (1993). *Phys. Rev. A*, **48**, 3906–3909.

Jackson, J. D. (1962). *Classical Electrodynamics.* New York: John Wiley and Sons.

Knox, W. H. (1988). *IEEE J. Quantum Electron.* **24**, 388–397.

Kohlweyer, S., Tsakiris, G. D., Wahlström, C.-G., Tillman, C. & Mercer, I. (1995). *Opt. Commun.* **117**, 431–438.

Linde, D. von der, Engers, T., Jenke, E., Agostini, P., Grillon, G., Nibbering, E., Mysyrowicz, A. & Antonetti, A. (1995). *Phys. Rev. A*, **52**, R25–27.

Lindenberg, A. M., Kang, I., Johnson, S. L., Missalla, T., Heimann, P. A., Chang, Z., Larsson, J., Bucksbaum, P. H., Kapteyn, H. C., Padmore, H. A., Lee, R. W., Wark, J. S. & Falcone, R. W. (2000). *Phys. Rev. Lett.* **84**, 111–114.

Moran, M. J. (1992). *Phys. Rev. Lett.* **69**, 2523–2526.

Norreys, P. A., Zepf, M., Moustaizis, S., Fews, A. P., Zhang, J., Lee, P., Bakarezos, M., Danson, C. N., Dyson, A., Gibbon, P., Loukakos, P., Neely, D., Walsh, F. N., Wark, J. S. & Dangor, A. E. (1996). *Phys. Rev. Lett.* **76**, 1832–1835.

Ondarza, R. (1998). *Rev. Mex. Fís.* **44**, 55–64.

Ondarza, R. (2001). *IEEE Trans. Plasma Sci.* To be published.

Pettifor, D. G. (1983). *Physical Metallurgy*. Amsterdam: North Holland.

Rolland, C. & Corkum, P. B. (1986). *J. Opt. Soc. Am. B*, **3**, 1625–1629.

Rose-Petruck, C., Jiménez, R., Guo, T., Cavalleri, A., Siders, C. W., Rksi, F., Squier, J. A., Walker, B. C., Wilson, K. R. & Barty, C. P. J. (1999). *Nature (London)*, **398**, 310–312.

Saeta, P., Wang, J.-K., Siegal, Y., Bloembergen, N. & Mazur, E. (1991). *Phys. Rev. Lett.* **67**, 1023–1026.

Salisbury, W. (1953). US Patent 2634372.

Shank, C. V., Yen, R. & Hirlimann, C. (1983). *Phys. Rev. Lett.* **50**, 454–457.

Silvestrelli, P. L., Alavi, A., Parrinello, M. & Frenkel, D. (1996). *Phys. Rev. Lett.* **77**, 3149–3152.

Smith, S. J. & Purcell, E. M. (1953). *Phys. Rev.* **92**, 1069.

Sokolowski-Tinten, K., Solis, J., Bialkowski, J., Siegel, J., Alfonso, C. N. & von der Linde, D. (1998). *Phys. Rev. Lett.* **81**, 3679–3682.

Tom, H. W. K., Aumiller, G. D. & Brito-Cruz, C. H. (1988). *Phys. Rev. Lett.* **60**, 1438–1441.

Tom, H. W. K., Mate, C. M., Zhu, X. D., Crowell, J. E., Heinz, T. F., Somorjai, G. A. & Shen, Y. R. (1984). *Phys. Rev. Lett.* **52**, 348–351.

Wales, D. J. (1996). *Science*, **271**, 925–929.

Wang, Z. L. (1998). *Adv. Mater.* **10**, 13–30.

Williams, D. B. & Carter, C. B. (1996). *Transmission Electron Microscopy*. New York/London: Plenum Press.

Ziman, J. M. (1972). *Principles of the Theory of Solids*. Cambridge University Press.